AD-A118 351 CALIFORNIA UNIV BERKELEY F/G 20/5
STUDIES OF SEMICONDUCTOR LASERS OF THE INTERFEROMETRIC AND RING--ETC(U)
SEP 81 S WANG, H K CHOI, I H FATTAH DAAG29-80-K-0011
UNCLASSIFIED ARO-17103.2-EL NL

END
DATE FILMED
9-82
DTIC

Studies of Semiconductor Lasers of the Interferometric and Ring Types

SHYH WANG, FELLOW, IEEE, HONG K. CHOI, STUDENT MEMBER, IEEE, AND ISMAIL H. A. FATTAH, STUDENT MEMBER, IEEE

Abstract—In this paper we present an analysis of semiconductor lasers of the interferometric and ring types, using the scattering-matrix formulation. The purpose of our analysis is to find new applications for semiconductor lasers beyond serving merely as a source for coherent radiation. Potential applications include wavelength stability, possibility for wavelength tuning and switching, operation as a traveling wave laser, and possible reduction in feedback effect. An initial set of experiments has been carried out and the results have borne out some theoretical predictions. These lasers should offer promises for use in integrated optics and fiber optical communication. Furthermore, the scattering-matrix formulation should be useful in treating other complex laser structures and lasers in an optical network environment.

I. Introduction

During the past few years, spectacular progress has been made in semiconductor lasers in achieving linear light-current characteristics, stable far-field radiation patterns, and single longitudinal-mode operation [1]. However, most of the research effort has been focused on lasers with a simple optical cavity of the Fabry-Perot type. In order to explore new applications for semiconductor lasers and to extend microwave techniques to guided-wave optics, it becomes necessary that we study lasers with complex structures for performing functions other than merely providing coherent radiation.

The purpose of this paper is twofold. First, we propose two specific laser structures [2], the interferometric laser for wavelength selection, and the ring laser for traveling-wave operation. Second, we demonstrate the usefulness of the scattering-matrix formulation in analyzing complex laser structures. As optical guided-wave technology evolves, we expect that functional demands will require laser structures other than the simple Fabry-Perot type and that a semiconductor laser can no longer be considered as a single entity by itself but should be treated as one component with possible interactions with other components in a complex optical system. These considerations inevitably lead to the use of techniques of circuit analysis. It seems natural that we look to microwave network theory for the analytical tools. One of the powerful techniques is the scattering-matrix formulation of networks [3], [4]. In this paper, we use the scattering-matrix formulation in analyzing the interferometric laser and the ring laser.

The results obtained for the two lasers are very encouraging. In the case of the interferometric laser, the longitudinal-mode behavior is shown to be very different from that in the simple Fabry-Perot laser. Possible applications of the interferometric laser for wavelength tuning and wavelength switching will be discussed. In the case of the ring laser, ways to minimize the coupling between the two counterrunning waves are indicated from the analysis. Discussions on possible benefits from this reduction, such as reducing the feedback effect, will be presented. Although our work is only a beginning, we hope that it may stimulate interest in developing other complex semiconductor laser structures and in analyzing the laser in its use involving other optical components in integrated optics and fiber optical communication.

II. The Scattering-Matrix Formulation

Consider a waveguide junction consisting of N-ports. If a_i and b_i with $i = 1, 2, \cdots, N$ represent, respectively, the amplitude of the wave propagating toward and away from the junction in port i, then the relation among the b's and a's can be represented by a scattering matrix with matrix element S_{ij} as $[b] = [S]\ [a]$ or in a set of simultaneous equations as

$$b_i = \sum S_{ij} a_j. \tag{1}$$

Based on considerations of the physical properties of the junction, we can derive certain conclusions about the scattering matrix. If the junction satisfies reciprocity, as is the case for waveguides devoid of magnetooptic effects then

$$S_{ij} = S_{ji}. \tag{2}$$

If the junction is loss free, power conservation requires that the matrix is also unitary, that is,

$$\sum_{i=1}^{N} S_{ij} S_{ik}^{*} = \delta_{jk}. \tag{3}$$

We should point out that in the scattering-matrix formulation, each port actually represents a given normal mode in a certain waveguide. Therefore, the number of ports generally exceeds the number of waveguides. It is especially important that the relevant radiation mode be included in the formulation. A case in point is an ideal Y junction. Suppose that the three guides support only the fundamental transverse mode. Let us further label the mode in the two input guides by $i = 2$ and 3, and the mode in the output guide by $i = 1$. Consider

Manuscript received September 1, 1981. This work was supported in part by the U.S. Army Research Office under Contract DAAG29-80-K-0011, the National Science Foundation under Grant ECS-8105208, and the U.S. Air Force Office of Scientific Research under Contract F49620-79-C-0178.

The authors are with the Department of Electrical Engineering and Computer Science and the Electronics Research Laboratory, University of California, Berkeley, CA 94720.

0018-9197/82/0400-0610$00.75

the situation in which the two waves propagating toward the junction in the two input guides are out of phase, that is, $a_2 = -a_3$ and $a_1 = 0$. If we limit the number of ports N to 3, we would find $S_{22} = S_{33} = -S_{23} = \frac{1}{2}$, $S_{12} = S_{13} = 1/\sqrt{2}$, $b_2 = a_2$, $b_3 = a_3$, and $b_1 = 0$ to be a solution of (1). Physically, we see that since the combined field of a_2 and a_3 in the case $a_2 = -a_3$ forms a higher order mode which cannot be supported by the output guide, conservation of energy would require that the two waves a_2 and a_3 be totally reflected.

The important point here is that, for a 3-port junction, we must include the radiation mode of the output guide in our formulation. A dielectric Y-junction, therefore, should be represented by a 4-port network even though we are dealing only with 3-port single-mode waveguides. The radiation mode of the output waveguide constitutes the fourth port. Therefore, the behaviors of both the interferometric laser and the ring laser will be analyzed using a 4×4 matrix. These two lasers are chosen for analysis because they represent the simplest examples of complex laser structures. From the two examples, we hope to gain some insight into the physical processes involved.

III. The Interferometric Laser

Many techniques presently used in guided-wave optics are already well developed, and can be readily borrowed from microwaves. One circuit element used extensively in microwaves but conspicuously missing in guided-wave optics is a tuning element. We propose to use a branching waveguide as an optical tuning element and to incorporate it in a semiconductor laser for longitudinal mode selection. Once we know how to provide a wavelength-selective mechanism in a laser structure, we can explore other possible uses for the laser, such as in FM, heterodyne, and multiplexing applications as well as potential benefits of the laser such as wavelength stability.

Consider the laser structure shown in Fig. 1(a) in the form of a fork. As mentioned earlier, many lasers have been developed showing single-mode operation. It is, therefore, practical to assume that the guiding structure of the interferometric laser supports only the fundamental transverse and lateral mode. In Fig. 1(a), the fields a_i and b_i refer to the fundamental mode in the three guides $i = 1$, 2, and 3 while the fields a_4 and b_4 represent the radiation mode of the guide 1. When the two incident fields a_2 and a_3 are not completely in phase, their out-of-phase components combine to form b_4. It is the interference between a_2 and a_3 which provides the mechanism for longitudinal mode selection. This problem is similar to the one treated by Rigrod and DiDomenico for gas lasers employing resonators of the open-ended Michelson-interferometer type [5], [6]. The scattering-matrix formalism is used here because it is general so that its application and hence our analysis can be extended to resonators of nonideal Michelson type as well as to other multiport resonators such as the ring resonator.

The threshold condition for the laser can be obtained by letting the inputs [I] be zero but the outputs [O] be nonzero at the three laser-exit facets [Fig. 2(a)]. Thus, we have at the laser facet

$$a_i' = R_i b_i' \tag{4}$$

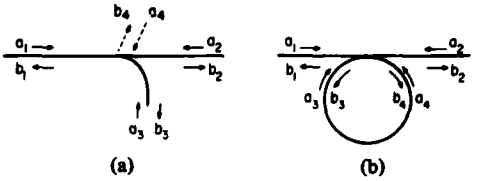

Fig. 1. Schematic diagram showing the structure of, and the fields in, (a) an interferometric laser and (b) a ring laser.

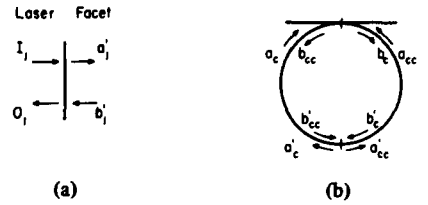

Fig. 2. Diagram showing (a) the fields at a laser facet and (b) the fields in a ring cavity expressed in terms of the clockwise mode and the counterclockwise mode.

and at the junction

$$a_i = R_i P_i^2 b_i \tag{5}$$

where R_i is the facet reflection coefficient, $P_i = \exp(\Gamma_i l_i) = g_i \exp(ik_i l_i)$ is the propagation factor, Γ_i the propagation constant, l_i the length, k_i the phase constant, and g_i the gain in the guide $i = 1$, 2, or 3. Substituting (5) into (1) and eliminating a_i, we obtain a characteristic equation of the following type:

$$[S'][b] = 0. \tag{6}$$

In the open-ended configuration of the Michelson interferometer, $R_4 = 0$ and $a_4 = 0$. In other words, the fourth port only contributes to loss and is not a part of the laser cavity. Therefore, only a 3×3 matrix $[S']$ results in the laser characteristic equation, (6). For nontrivial solutions, the determinant $|S'|$ must be zero, that is,

$$\begin{vmatrix} -1 & S_{12}P_2^2R_2 & S_{13}P_3^2R_3 \\ S_{21}P_1^2R_1 & -1 & 0 \\ S_{31}P_1^2R_1 & 0 & -1 \end{vmatrix} = 0. \tag{7}$$

In (7) we have neglected interscattering between guides 2 and 3 and reflections back into the guides by setting $S_{23} = S_{32} = 0$ and $S_{ii} = 0$. These conditions can be met if the fork angle is small and the transition from a single guide into two guides is gradual. Under closely phase-matched conditions $k_1 = k_2 = k_3$ at the junction, only the matrix elements $S_{13} = S_{31}$ and $S_{12} = S_{21}$ have appreciable magnitudes. Expanding (7) and rearranging terms, we can express the oscillation condition in a form commonly used for Fabry-Perot lasers as follows

$$R_{eff}^2 \exp 2(\Gamma_1 l_1 + \Gamma_2 l_2) = 1 \tag{8}$$

where R_{eff}^2 is the effective reflectance given by

$$R_{eff}^2 = R_1 R_2 |S_{12}|^2 [1 + A \exp(i\theta)] \tag{9}$$

and

$$A \exp(i\theta) = (S_{13}/S_{12})^2 (R_3/R_2)(P_3/P_2)^2.$$

Obviously, the value of R_{eff}^2 reaches a maximum and hence the threshold gain is a minimum when both cavities $l_1 + l_2$ and $l_1 + l_3$ are in resonance; that is,

$$\theta_{12} = 4\pi n(l_1 + l_2)/\lambda = m_{12}\,2\pi \tag{10}$$

$$\theta_{13} = 4\pi n(l_1 + l_3)/\lambda = m_{13}\,2\pi \tag{11}$$

where n is the effective guide index and m_{12} and m_{13} are integers. To have a feel of the magnitude of the interference effect, we make a numerical calculation of R_{eff}^2. For semiconductor lasers unlike gas lasers, it is impractical to build an ideal 3 dB beam splitter into the laser structure. Instead we assume $|S_{12}|^2 = 0.75$ and $|S_{13}|^2 = 0.15$ for a 10 percent insertion loss at the junction. In Fig. 3, the value of $|R_{eff}|^2/R_1R_2$ is plotted as a function of wavelength (solid upper curve). The length $l_2 - l_3$ (about 170 μm) is so chosen that the spacing between successive values of $\theta = \theta_{12} - \theta_{13}$ being multiples of 2π is 6 Å at 8650 Å, and the value of A in (9) is assumed 0.2.

Several features of the $|R_{eff}|^2$ curve are worth noting. First, the variation of $|R_{eff}|^2$ is comparable to the difference in facet reflectance calculated for guide TE and TM waves [7], and hence should be sufficient to suppress modes away from maximum $|R_{eff}|^2$. Had we used a value for A close to 1 for an ideal 3 dB beam splitter, large ratio of maximum to minimum $|R_{eff}|^2$ would be obtained. Second, to provide effective discrimination of neighboring longitudinal modes, the phase difference θ should change appreciably over the longitudinal mode spacing. In other words, the path difference $l_2 - l_3$ should be sufficiently large, on the order of 100 μm. On the other hand, if R_{eff} undergoes several cycles of oscillation from maxima to minima between two neighboring modes then longitudinal mode discrimination would no longer be effective. This would happen if $l_2 - l_3 > 500$ μm.

Another way of seeing the interference effect on the laser is to examine the ratio of the outgoing and incoming power at the junction. The quantity

$$LF = 1 - |b_1|^2/(|a_2|^2 + |a_3|^2) \tag{12}$$

can be considered as the loss factor of the junction. The ratio $b_2/b_3 = S_{12}/S_{13}$ can be found from the cofactors of $[S']$. Using this ratio in (5) and (12), we find

$$LF = 1 - |S_{12}|^2\,\frac{|1 + A\exp(i\theta)|^2}{1 + A^2\,|S_{12}/S_{13}|^2}. \tag{13}$$

In Fig. 3, the value of LF is also plotted as a function of wavelength (lower dashed curve). If the two incident fields a_2 and a_3 at the junction are out of phase, some of the incident power is lost to the radiation mode (port 4), resulting in increased loss. For an ideal 3 dB beam splitter, $S_{12}^2 = S_{13}^2 = \frac{1}{2}$ and $A = 1$. These values yield a maximum $LF = 1$ and a minimum $R_{eff}^2 = 0$ when $\theta = \pi$.

To determine the longitudinal modes of the composite cavity, we must examine quantities other than R_{eff}^2 and FL. The laser oscillation conditon as stated in (7) can be separated into real and imaginary parts. The imaginary part is given by

$$|S_{12}|^2R_1R_2g_1g_2\sin\theta_{12} + |S_{13}|^2R_1R_3g_1g_3\sin\theta_{13} = 0 \tag{14}$$

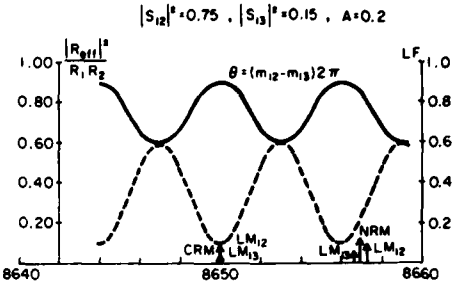

Fig. 3. Diagram showing the variations of the effective reflectance $|R_{eff}|^2/R_1R_2$ (upper solid curve) and the loss factor LF (lower dashed curve) as function of wavelength.

where g_i is the gain in guide i, and the real part is given by

$$|S_{12}|^2R_1R_2g_1g_2\cos\theta_{12} + |S_{13}|^2R_1R_3g_1g_3\cos\theta_{13} = 1. \tag{15}$$

Since the quantities in front of $\sin\theta_{12}$ and $\sin\theta_{13}$ in (14) are all positive, there are only two possible types of solutions to (14): one with $\sin\theta_{12} = \sin\theta_{13} = 0$ and the other with $\sin\theta_{12}$ and $\sin\theta_{13}$ having opposite signs.

Accordingly, the longitudinal modes of the interferometric laser can be classified into two groups: the coincidence resonance mode and the nonresonance mode. For $\sin\theta_{12} = \sin\theta_{13} = 0$, both (6) and (7) are satisfied. In other words, the two cavities $l_1 + l_2$ and $l_1 + l_3$ are in resonance simultaneously at the wavelength λ. This case is referred to as the coincidence resonance mode and indicated by CRM in Fig. 3. The CRM is assumed to be located at $\lambda = 8650$ Å. For the CRM, θ is an integral multiple of 2π; therefore, R_{eff}^2 is a maximum and LF is a minimum. However, the converse is not always true because maximum R_{eff}^2 and minimum LF do not guarantee the simultaneous satisfaction of (10) and (11). This fact means that the CRM's are further apart in wavelength than the maxima of R_{eff}^2.

In between two neighboring CRM's lie the nonresonant modes which are indicated by NRM in Fig. 3. Note that (14) can still be satisfied with $\sin\theta_{12}$ and $\sin\theta_{13}$ having opposite signs. If LM_{12} and LM_{13} denote the longitudinal mode of the cavity $l_1 + l_2$ and that of the cavity $l_1 + l_3$, respectively, then the longitudinal mode of the composite cavity LM has to be between LM_{12} and LM_{13}. For nonzero $\sin\theta_{12}$ and $\sin\theta_{13}$, $\cos\theta_{12}$ and $\cos\theta_{13}$ are smaller than 1 leading to a higher threshold gain from (15). Since $\sin\theta_{12}$ and $\sin\theta_{13}$ must have opposite signs, θ can no longer be an integral multiple of 2π. This means that the NRM's will have their fields a_2 and a_3 out of phase at the junction and hence a higher threshold gain than the CRM's.

To test the theory, we have fabricated two groups of oxide, stripe-geometry lasers of 10 μm stripe width: one group being the straight Fabry-Perot laser and the other group being the interferometric laser of the type shown in Fig. 1(a). The spectrum of a straight laser is shown in Fig. 4 and that of an interferometric laser is shown in Fig. 5. Several distinct characteristics have been observed and can be summarized as follows. The straight lasers show simultaneous oscillations of many longitudinal modes whose intensity profile follows more or

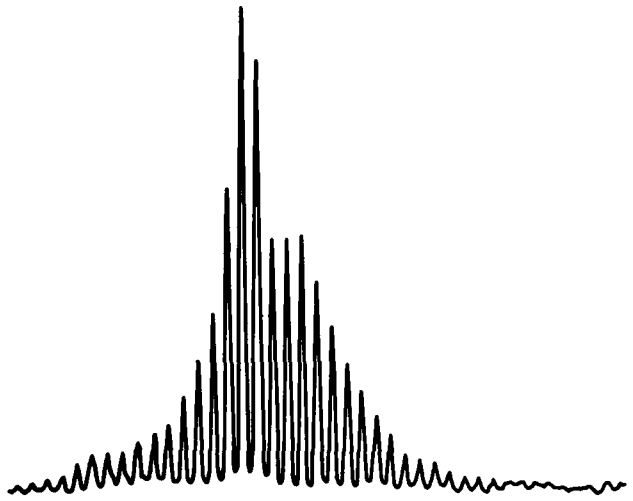

Fig. 4. The lasing spectrum of a Fabry-Perot oxide-stripe laser.

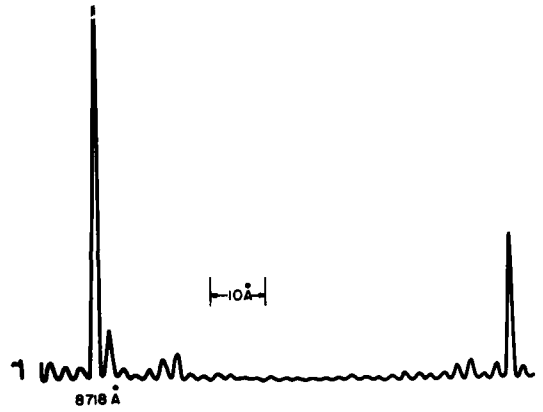

Fig. 5. The lasing spectrum of an interferometric oxide-stripe laser.

less the spontaneous emission profile. The interferometric lasers, on the other hand, show either one dominant longitudinal mode or a limited number of dominant longitudinal modes which are far apart. In Fig. 5, we see that the two dominant modes are about 70 Å apart.

We should also point out that the interferometric lasers generally oscillate at a wavelength away from the peak of the spontaneous emission. At low injection currents, the interferometric lasers oscillate in a single mode. When the injection current is sufficiently high, a satellite group of longitudinal modes begins to appear around a wavelength ranging from few tens to one hundred angstroms away from the main group as shown in Fig. 5. Sometimes there are several modes in the main and satellite groups. Even when this multimode behavior shows in each group, the two groups remain distinct and maintain the same separation in wavelength.

Qualitatively, the behaviors of the interferometric laser can be understood on the basis of reflectance and loss modulation shown in Fig. 3. Obviously, the two modes shown in Fig. 5 are both coincidence resonance modes. However, the possibility of three-cavity interference effects can not be ruled out. In the analysis presented here, we have neglected reflections back into the original guide. For sufficiently large matrix elements S_{ii}, the interferometric laser is best described by three cavities, l_1, l_2, and l_3, and hence expected to lase at a wavelength where all the three cavities are in resonance. This possibility requires further investigation.

IV. The Ring Laser

A semiconductor ring laser possesses many interesting and advantageous potentials for uses in integrated optics and fiber optical communication. First, it does not require a mirror so it should be readily integrable with other components in an integrated optical circuit based on GaAs and related semiconductor technology. Second, it offers the possibility [2] of reducing the feedback effect if we can find ways of operating the laser in predominantly traveling-wave modes. The operation of a diode ring laser of the high mesa type [8] has been reported recently. The main purpose of the present discussion is to analyze the operation of a semiconductor ring laser using the scattering-matrix formulation. Through the analysis, we hope to gain some insight into how to minimize the effects of facet and junction reflection and thus to achieve laser operation predominantly in traveling-wave modes.

Consider the ring laser structure shown in Fig. 1(b), which consists of a circular waveguide and two branching straight waveguides serving as two output arms. Here we choose a circular guide instead of a race-track-type guide for the following reason. Our experience with half-ring lasers [9] made of a half circle and two straight sections indicates that a significant amount of mode conversion and reflection takes place at the junction between a circular guide and a straight guide. It is well known that the field in a circular guide tends toward the outer periphery of the guide. Therefore, there is an appreciable mismatch of the field distribution at the junction of a circular and straight guide. The use of a circular guide instead of a race-track guide eliminates internal reflection and mode conversion within the laser cavity itself. It is true that reflections still exist at the junction of the ring cavity and the two output guides. However, the coupling between the output guides and the ring cavity is weak. Therefore, reflections at the junction are expected to be much less significant and hence much less detrimental than internal reflections.

The fields in the ring cavity and the two output arms of Fig. 1(b) are related to each other by conventional 4×4 S matrix. However, for the ring cavity, it is more convenient to refer to the fields a_c, b_c, a_{cc}, and b_{cc} associated with the clockwise the counterclockwise traveling wave modes [as shown in Fig. 2(b)] than to the fields a_3, b_3, a_4, and b_4 associated with each branch waveguide [as shown in Fig. 1(b)]. Recognizing that $a_c = a_3$, $b_c = b_4$, $a_{cc} = a_4$, and $b_{cc} = b_3$, we have the following relation at the upper junction

$$\begin{bmatrix} b_1 \\ b_2 \\ b_c \\ b_{cc} \end{bmatrix} = \begin{bmatrix} S_{11} & S_{12} & S_{13} & S_{14} \\ S_{21} & S_{22} & S_{23} & S_{24} \\ S_{31} & S_{32} & S_{33} & S_{34} \\ S_{41} & S_{42} & S_{43} & S_{44} \end{bmatrix} \begin{bmatrix} a_1 \\ a_2 \\ a_c \\ a_{cc} \end{bmatrix} \tag{16}$$

Because of the interchange of the subscripts, reciprocity at the junction now requires

$$S_{12} = S_{21}, \quad S_{13} = S_{41}, \quad S_{24} = S_{32} \tag{17}$$

$$S_{33} = S_{44}, \quad S_{14} = S_{31}, \quad S_{23} = S_{42}. \tag{18}$$

The laser oscillation condition can be obtained as follows. At the lower junction in Fig. 2(b), the ring cavity simply runs into itself without any branching. Therefore, we have

$$a_c' = b_c' \quad \text{and} \quad a_{cc}' = b_{cc}' \tag{19}$$

which leads to

$$a_c = b_c P_R^2 \quad \text{and} \quad a_{cc} = b_{cc} P_R^2 \tag{20}$$

where $P_R = g_R \exp(ik_R \pi r)$ is the propagation factor for one-half of the ring. If there are no inputs ($I_{1,2} = 0$) at the facets of the two output arms, then the fields in the two straight guides are related by

$$a_i = b_i R_i P_i^2 \quad \text{with} \quad i = 1 \text{ or } 2. \tag{21}$$

Substituting (20) and (21) into (16), and eliminating a_i, we find the characteristic equation $[S']\ [b] = 0$ for the laser. However, the laser scattering matrix $[S']$ contains too many terms which make physical interpretation of the results difficult.

To facilitate identifying physical processes that couple the two counterrunning traveling wave modes, we make the following simplifying assumptions. First, the coupling between waves moving in opposite directions in two guides, for example, between a_1 and b_{cc}, is small. Thus, we let

$$S_{32} = S_{41} = S_{24} = S_{13} = 0. \tag{22}$$

Second, the coupling between the straight guides and the circular guide is weak so that reflection of a wave back into the original guide is small. Thus, we further let

$$S_{11} = S_{22} = S_{34} = S_{43} = 0. \tag{23}$$

With the above simplifications, the laser characteristic equation $|S'| = 0$ becomes

$$\begin{bmatrix} -1 & S_{12}R_2P_2^2 & 0 & S_{14}P_R^2 \\ S_{21}R_1P_1^2 & -1 & S_{23}P_R^2 & 0 \\ S_{31}R_1P_1^2 & 0 & S_{33}P_R^2 - 1 & 0 \\ 0 & S_{42}R_2P_2^2 & 0 & S_{44}P_R^2 - 1 \end{bmatrix} = 0. \tag{24}$$

Expanding (24), we obtain

$$xyz = xu + yv + w \tag{25}$$

where the various quantities are given by

$$x = 1 - S_{33}P_R^2 \tag{26}$$

$$Y = 1 - S_{44}P_R^2 \tag{27}$$

$$z = 1 - S_{12}^2 R_1 R_2 P_1^2 P_2^2 \tag{28}$$

$$u = S_{12}R_2P_2^2 S_{23}P_R^2 S_{31}R_1P_1^2 \tag{29}$$

$$v = S_{21}R_1P_1^2 S_{14}P_R^2 S_{42}R_2P_2^2 \tag{30}$$

$$w = S_{14}P_R^2 S_{23}P_R^2 S_{42} S_{31}R_1R_2P_1^2P_2^2. \tag{31}$$

If there is no coupling between the straight guide and the ring cavity, $u = v = w = 0$ and the solutions of the characteristic equation are

$$x = 0, \quad y = 0, \quad \text{and} \quad z = 0 \tag{32}$$

which represent, respectively, the two counterrunning traveling wave modes of the ring cavity and the Fabry-Perot mode of the combined straight guide. For weak coupling between the straight guide and the ring cavity, the three quantities on the right-hand side of (25) can be treated as perturbations which couple the normal modes of the ring cavity to the Fabry-Perot mode of the straight guide.

There are several ways of arranging the terms in (25). In Fig. 6, we show the six possible closed loops representing the following: (a) $x = 0$, the clockwise mode; (b) $y = 0$, the counterclockwise mode; (c) $z = 0$, the Fabry-Perot mode; (d) $u = 1$ and (e) $v = 1$, a combination mode involving one single circular (clockwise for $u = 1$ and counterclockwise for $v = 1$) pass and one complete pass in the straight guide; and (f) $w = 1$, a combination mode involving two passes (one clockwise and one counterclockwise) in the ring cavity and one complete pass in the straight guide. In (25) the arrangement is so that the dominant modes of the composite cavity are represented by $x = 0$, $y = 0$, and $z = 0$. It is interesting to note that reciprocity demands a symmetrical form of the characteristic equation for the two counterrunning traveling wave modes. Therefore, in the absence of a nonreciprocal element in the ring cavity, the clockwise and counterclockwise modes are excited simultaneously. The important question is the relative amplitude of the two counterrunning waves. It is the purpose of our analysis to find ways to make the ratio b_c/b_{cc} large so that the laser can operate in one predominant traveling-wave mode.

It is interesting to note from (25) that if we make one output arm, say guide 2 in Fig. 1(a), highly absorbing or reduce facet reflectance R_2, the quantities u, v, and w all become very small, and then the three modes $x = 0$, $y = 0$, and $z = 0$ become almost decoupled. The next logical step in our analysis is to let $a_2 = 0$ but keep $b_2 \neq 0$. Furthermore, we introduce the reflection at the junction S_{34} and S_{43} into the formulation. Since $a_2 = 0$, the lasing condition is determined by a 3×3 determinant involving b_1, b_c, and b_{cc} as follows:

$$\begin{bmatrix} -1 & 0 & S_{14}P_R^2 \\ S_{31}R_1P_1^2 & S_{33}P_R^2 - 1 & S_{34}P_R^2 \\ 0 & S_{43}P_4^2 & S_{44}P_R^2 - 1 \end{bmatrix} \begin{bmatrix} b_1 \\ b_c \\ b_{cc} \end{bmatrix} = 0. \tag{33}$$

For simplicity, in (33), we only include the most important interaction, as represented by S_{34} and S_{43}, which directly couples the two counterrunning waves. The assumption specified in (22) is still kept.

Expanding (33), we find

$$(1 - S_{33}P_R^2)(1 - S_{44}P_R^2) - B^2P_R^4 = 0 \tag{34}$$

where the parameter B is given by

$$B^2 = S_{14}S_{43}S_{31}R_1P_1^2 + S_{34}S_{43}. \tag{35}$$

Since $S_{33} = S_{44}$, the two solutions of (34) are

$$(S_{33} + B)P_4^2 = 1 \tag{36}$$

$$(S_{33} - B)P_R^2 = 1. \tag{37}$$

Obviously, the solution of (36) has a lower threshold gain than that of (37). Furthermore, the threshold reaches a minimum when P_1^2 is a real and positive number and equal to g_1^2. The in-

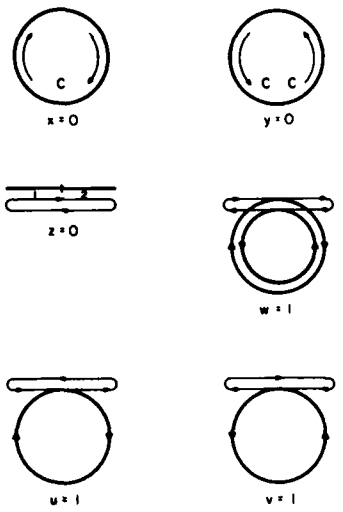

Fig. 6. Schematic diagram showing the six possible lasing loops in a ring laser with two straight output arms.

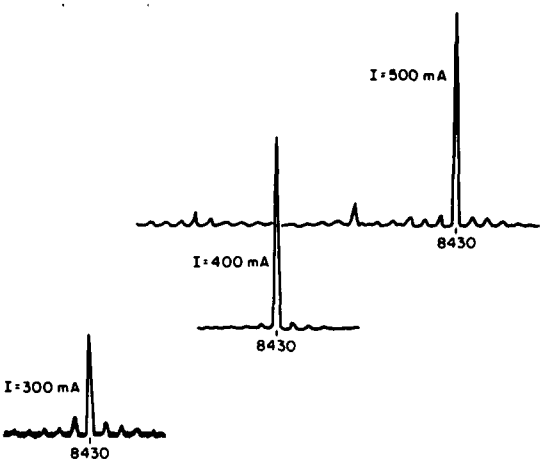

Fig. 7. The lasing spectra of a high-mesa ring laser.

terference between the wave caused by reflection at the junction as represented by the term $S_{34}S_{43}$ in B^2 and the wave caused by reflection at the facet as represented by the term involving $R_1P_1^2$ in B^2 provides the mechanism for longitudinal mode selection. Therefore, the lasing wavelength is determined by the simultaneous satisfaction of the resonance conditions of the ring cavity and the straight guide 1

$$2\pi k_R r = m_R 2\pi \tag{38}$$

$$2k_1 l_1 = m_1 2\pi \tag{39}$$

where m_R and m_1 are two integers.

The ratio b_c/b_{cc} can be obtained from the third equation of (33) and is found to be

$$\frac{b_c}{b_{cc}} = \frac{S_{44}P_R^2 - 1}{-S_{43}P_R^2} = \frac{B}{S_{43}}. \tag{40}$$

As mentioned earlier, the lowest threshold is reached when the two terms in (35) are additive. Therefore, B is always larger than S_{43}. The first term in B^2 of (35) represents coupling of the counterclockwise wave to the arm 1 (as represented by S_{14}) followed by reflection at the facet and then coupling back into the ring cavity as a clockwise wave (as represented by S_{31}). It is this constant conversion of the counterclockwise wave into the clockwise wave which makes $b_c > b_{cc}$. The maximum ratio achievable, limited by the threshold condition of arm 1, is expected to be on the order of $(S_{14}S_{31}/S_{11}S_{34})^{1/2}$ which can be made quite large.

In Fig. 7, the spectra of a high-mesa oxide-stripe injection ring laser are shown at several injection currents. The ring laser consists of two output arms of which one is pumped and the other is unpumped. The high loss in the unpumped region has several consequences. First, $P_1^2 = 0$ makes the above analysis applicable. Second, it prevents the Fabry-Perot mode of the straight guide from lasing. Third, the spectrum can be measured only through the output arm with $R_2P_2^2 \neq 0$. The ring laser has a radius of 100 μm, and a total pumped region of about 800 μm. The threshold current of 280 mA is quite reasonable, considering the overall length and a stripe width of 12 μm. Although the circular guide can support many lateral modes due to the high index difference of the high mesa structure, the laser operates predominately in a single longitudinal mode and the lasing wavelength stays at 8430 Å even at higher injection currents. We believe that the interference effect built into the laser structure has helped not only in promoting single-mode operation but also in maintaining wavelength stability.

V. Discussion of Potential Applications

Thus far, the experiments on the interferometric laser and the ring laser have been performed in structures which are simple to fabricate, such as the oxide-stripe and the high-mesa types, but whose guiding property in the lateral direction is not the most suitable for the two lasers. Even so, the initial experimental results on the two lasers have been very encouraging. In this section, we discuss some potential applications of the two lasers.

For the interferometric laser, our discussion will be focused on controlling the laser wavelength. If we use a large optical cavity in a monolithic laser structure or a combination of $LiNbO_3$ and semiconductor guides in a hybrid laser structure, we can have many different combinations of active and passive elements in the laser structure [5], [10]. The passive element can be used for electrooptic tuning of the laser wavelength. When the electrooptic effect is applied to the common arm 1 alone [Fig. 1(a)] or when the electrooptic effect is applied to both branches 2 and 3 to produce index changes in the ratio

$$\frac{\Delta n_2}{\Delta n_3} = \frac{l_3(n_1 l_1 + n_2 l_2)}{l_2(n_1 l_1 + n_3 l_3)} \tag{41}$$

the two resonance conditions stated in (10) and (11) will move together, resulting in a continuous shift in wavelength of the coincidence resonance mode. The situation is illustrated in Fig. 8(a). On the other hand, since LM_{12} and LM_{13} move by the same amount in its location, the NRM's remain as NRM's and hence are not expected to lase.

The range of continuous tuning will be limited by the maximum field that can be applied across the guide, and hence

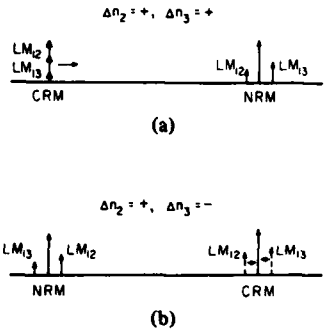

Fig. 8. Schematic diagram illustrating the arrangements for (a) continuous tuning and (b) wavelength switching of an interferometric laser.

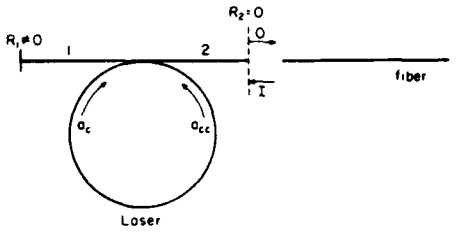

Fig. 9. Schematic diagram showing a ring laser coupled to a fiber. Arm 2 with $R_2 = 0$ is for power output while arm 1 with a finite R_1 is for monitoring.

should be small, probably on the order of a few angstroms. In certain future possible applications, a small amount of tunability should be sufficient. For example, in FM, a modulation of wavelength by 1 Å already means a bandwidth of 30 GHz at $\lambda = 1$ μm. In heterodyne detection, fine tuning will be needed to keep a laser wavelength identical to that of a local oscillator. The schemes proposed for continuous tuning could be used for fine tuning.

Another interesting possibility with the interferometric laser is wavelength switching which can cover a wide wavelength range comparable to the spontaneous emission bandwidth. The mechanism for wavelength switching is illustrated in Fig. 8(b). As discussed in Section III, our experimental results show that the interferometric laser is capable of oscillation over a wide range of the spontaneous emission spectrum. The exact location is determined by the coincidence of the two cavity modes. By properly choosing the applied voltage or voltages to shift the locations of LM_{12} and LM_{13}, for example, LM_{13} toward shorter wavelength and LM_{12} toward longer wavelength as shown in Fig. 8(b), we should be able to bring the coincidence resonance mode to a new wavelength few tens of angstroms away from the original laser wavelength without the applied voltage. Controlled wavelength switching should make it possible for a single semiconductor laser to serve as a multiple-wavelength source with one wavelength for each channel in future wavelength multiplexing. Since LM_{12} and LM_{13} move in opposite directions and since the spacing between two neighboring LM_{12} and LM_{13} is smaller than the spacing between two neighboring LM_{12} or neighboring LM_{13}, the voltage needed for controlled switching is expected to be less than that for continuous tuning.

Let us now turn our attention to the ring laser. Fig. 9 illustrates the laser configuration for use in conjunction with a fiber. One important result of our analysis is the possibility to operate the laser predominately in one traveling wave mode. It is this predominant mode which is coupled to the output arm with $R_2 = 0$. Obviously it should be possible to integrate the laser directly with other optical components. The fact $R_2 = 0$ also means that we could apply antireflection coating to facet 2. This should facilitate the use of a hybrid arrangement, such as an isolator, to reduce any optical feedback from a fiber. Note from (16) that the dominant terms for b_1 and b_2 are $b_1 = S_{14}a_{cc}$ and $b_2 = S_{23}a_c$. Since the ratio b_c/b_{cc} can be made large, the percentage of useful laser light to be coupled out through arm 2 is expected to be high. The small percentage of light coupled out through arm 1 could be used for monitoring purposes. A laser operating predominantly in one traveling wave also would render more uniform carrier distribution and thus be more amenable to single longitudinal-mode operation.

The effect of optical feedback can be examined through (16) by treating a_2 as an input and then solving for b_1, b_c, and b_{cc}. The important quantity is the ratio of b_c/b_{cc} which is found to be

$$\left(\frac{b_c}{b_{cc}}\right)_{FB} = \frac{S_{31}R_1P_1^2(S_{42}S_{14} - BS_{12}) - S_{42}S_{34}}{\cdot S_{42}B + S_{12}S_{31}S_{34}R_1P_1^2} \tag{42}$$

where the subscript FB refers to fields caused by feedback. Since B is real and positive, it should be possible to make this ratio zero by properly choosing $R_1P_1^2$. Under the circumstance, the output of the ring laser b_c should be little affected by the optical feedback. We should add, however, that the operating condition for minimum feedback effect may not result in a large ratio B/S_{43} in (40). In other words, there would be a compromise between reducing the feedback effect and operating the laser predominantly in one traveling wave mode. It is interesting to note that for both $R_2 = 0$ and $R_1 = 0$, (42) reduces to $(b_c)_{FB} = (b_{cc})_{FB}$ and a ring laser with nonzero $S_{34} = S_{43}$ behaves as a standing-wave laser. Therefore, the worst situation for a ring laser is the usual situation for a Fabry-Perot laser insofar as the effect of optical feedback is concerned.

Finally, we should point out that interference effect exists in both the interferometric laser of Fig. 1(a) and the ring laser in Fig. 1(b). The requirement of simultaneous satisfaction of (10) and (11) for the former and of (38) and (39) for the latter should improve temperature stability of the laser wavelength. For the simple Fabry-Perot laser, because of the lack of a wavelength-selection mechanism, the wavelength is determined by the peak of the spontaneous emission which changes appreciably with temperature at a rate of about 3 Å/K. By comparison, the rate of wavelength change in DBR lasers [11] which is mainly due to index and length changes has been reported only about 0.8 Å/K. The interferometric and ring lasers are expected to have a similar rate as the DBR laser because the factors affecting the simultaneous satisfaction of (10) and (11), or (38) and (39) are the temperature dependences of n and l. Since the modes from both equations move in the same direction, wavelength switching is not expected.

VI. Conclusion

In this paper, we have presented an analysis of the interferometric laser and the ring laser, using the scattering-matrix formulation. The lasers are shown to possess certain unique properties which are absent in the simple Fabry-Perot laser. The initial set of experiments has indeed borne out some of the theoretical predictions. Several potential applications have been discussed including wavelength stability, possibility for wavelength tuning and switching, operation as a traveling wave laser, and possible reduction in feedback effect. These represent new and exciting possibilities for semiconductor lasers.

References

[1] S. Wang, C. Y. Chen, A.S.H. Liao, and L. Figueroa, "Control of mode behavior in semiconductor lasers," *IEEE J. Quantum Electron.*, vol. QE-17, pp. 453-468, Aug. 1981 (see references).

[2] S. Wang, "Studies of novel semiconductor laser structures for integrated optics and optical fiber communication," presented at NSF Grantee-User Meet. on Opt. Commun. under E. Schutzman, Washington Univ., St. Louis, MO, May 27-29, 1981.

[3] R. N. Ghose, *Microwave Circuit Theory and Analysis*. New York: McGraw-Hill, 1963.

[4] C. G. Montgomery, R. H. Dicke, and E. M. Purcell, "Principles of microwave circuits," in *MIT Radiation Laboratory Series*, vol. 8. New York: McGraw-Hill, 1948.

[5] W. W. Rigrod, "Selectivity of open-ended interferometric resonators," *IEEE J. Quantum Electron.*, vol. QE-6, pp. 9-14, 1970.

[6] M. DiDomenico, "Characteristics of single-frequency Michelson-type He-Ne gas laser," *IEEE J. Quantum Electron.*, vol. QE-2, pp. 311-322, 1966.

[7] H. C. Casey, Jr. and M. B. Parish, *Heterostructure Lasers, part A*. New York: Academic, 1978, p. 80.

[8] A.S.H. Liao and S. Wang, "Semiconductor injection lasers with a circular resonator," *Appl. Phys. Lett.*, vol. 36, pp. 801-803, 1980.

[9] —, "Half-ring (GaAl)As double-heterojunction injection lasers," *Appl. Phys. Lett.*, vol. 36, pp. 353-356, 1980.

[10] P. W. Smith, "Mode selection in lasers," *Proc. IEEE*, vol. 60, pp. 422-440, 1972.

[11] H. Namizaki, M. K. Shams, and S. Wang, "Large-optical-cavity GaAs-(GaAl)As injection laser with low-loss distributed Bragg reflectors," *Appl. Phys. Lett.*, vol. 31, pp. 122-124, 1977.

Shyh Wang (M'57-SM'75-F'78), photograph and biography not available at the time of publication.

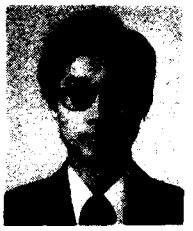

Hong K. Choi (S'74-M'76-S'80) was born in Kwangju, Korea, on July 30, 1951. He received the B.S. degree in electronic engineering from the Seoul National University, Seoul, Korea in 1973 and the M.S. degree in electrical engineering from the Korea Advanced Institute of Science and Technology, Seoul, Korea in 1975.

From 1975 to 1978, he worked at the Agency for Defense Development, Seoul, Korea. Since 1979, he has been working toward the Ph.D. degree in electrical engineering in the Depatment of Electrical Engineering and Computer Science, University of California, Berkeley, where he is working as a Research Assistant. His research interest is in semiconductor ring lasers and lasers using interference effects.

Mr. Choi is a student member of the Optical Society of America.

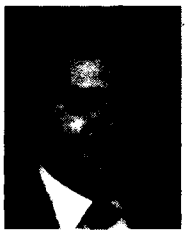

Ismail H. A. Fattah (S'79) was born in Cairo, Egypt, in 1953. He received the B.S. degree in electronic engineering with honors from Ain Shams University, Cairo, Egypt, in 1975, and the M.Eng. degree in electrical engineering from Tulane University, New Orleans, LA, in 1978.

He is currently working towards the Ph.D. degree in electrical engineering at the University of California, Berkeley. He worked as a Teaching and Research Assistant at the Department of Electrical Engineering, Ain Shams University, from 1975 to 1977. Since 1978 he has been a Teaching Assistant and a Research Assistant at the Department of Electrical Engineering and the Electronics Research Laboratory, University of California, Berkeley. His current interests are in semiconductor laser fabrication technology and its application to optical communications.

Mr. Fattah is a member of the Optical Society of America.

Unclassified

SECURITY CLASSIFICATION OF THIS PAGE (When Data Entered)

REPORT DOCUMENTATION PAGE		READ INSTRUCTIONS BEFORE COMPLETING FORM
1. REPORT NUMBER 17102.2-EL	2. GOVT ACCESSION NO. AD-A118351 N/A	3. RECIPIENT'S CATALOG NUMBER N/A
4. TITLE (and Subtitle) Studies of Semiconductor Lasers of the Interferometric and Ring Types		5. TYPE OF REPORT & PERIOD COVERED Reprint 6. PERFORMING ORG. REPORT NUMBER N/A
7. AUTHOR(s) Shyh Wang Hong K. Choi Ismail H. A. Fattah		8. CONTRACT OR GRANT NUMBER(s) DAAG29 80 K 0011
9. PERFORMING ORGANIZATION NAME AND ADDRESS University of California Berkeley, CA 94720		10. PROGRAM ELEMENT, PROJECT, TASK AREA & WORK UNIT NUMBERS N/A
11. CONTROLLING OFFICE NAME AND ADDRESS U. S. Army Research Office P. O. Box 12211 Research Triangle Park, NC 27709		12. REPORT DATE Apr 82 13. NUMBER OF PAGES 8
14. MONITORING AGENCY NAME & ADDRESS(if different from Controlling Office)		15. SECURITY CLASS. (of this report) Unclassified 15a. DECLASSIFICATION/DOWNGRADING SCHEDULE

16. DISTRIBUTION STATEMENT (of this Report)

Submitted for announcement only.

17. DISTRIBUTION STATEMENT (of the abstract entered in Block 20, if different from Report)

18. SUPPLEMENTARY NOTES

19. KEY WORDS (Continue on reverse side if necessary and identify by block number)

20. ABSTRACT (Continue on reverse side if necessary and identify by block number)

DD FORM 1 JAN 73 1473 EDITION OF 1 NOV 65 IS OBSOLETE

Unclassified

SECURITY CLASSIFICATION OF THIS PAGE (When Data Entered)